Churchill James H. (Orcid ID: 0000-0002-6497-810X)

Title: The Impact of Ocean Warming on Juvenile American Lobster Recruitment off Southeastern Massachusetts

Running Title: Ocean Warming and Lobster Recruitment

Authors: Flynn Casey[1] (flynn.casey.92@gmail.com)

James H. Churchill[2] (jchurchill@whoi.edu; orcid.org/0000-0002-6497-810X; corresponding author)

Geoffrey W. Cowles[1] (gcowles@umassd.edu)

Tracy L. Pugh[3] (tracy.pugh@state.ma.us)

Richard A. Wahle[4] (richard.wahle@maine.edu)

Kevin D.E. Stokesbury[1] (kstokesbury@umassd.edu)

Robert P. Glenn[3] (robert.glenn@state.ma.us)

[1]Dept. of Fisheries Oceanography, Sch. of Marine Sciences and Technology, University of Massachusetts Dartmouth, 836 S Rodney French Blvd, New Bedford, MA 02744, U.S.A.

[2]Dept. of Physical Oceanography, Woods Hole Oceanographic Inst., Woods Hole, MA 02543, U.S.A.

[3]Massachusetts Div. of Marine Fisheries, 836 S Rodney French Blvd, New Bedford, MA 02744, U.S.A.

[4] Sch. of Mar. Sci., University of Maine, Darling Marine Center, Walpole, ME 04573, U.S.A

Conflict of Interest Statement
The authors declare that there exist no conflicts of interest.

Data Availability Statement
All data provided by the Massachusetts Division of Marine Fisheries (MADMF) for the purpose of this study is available upon written request, which should be submitted to MADMF. NeCOFS ocean hindcast data is available using OpenDAP from http://www.smast.umassd.edu:8080/thredds/catalog.html.

Abstract

During the 1990s, coastal habitat off southeastern Massachusetts (SEMA) supported commercially viable fisheries for American lobster (*Homarus americanus*). Over the past two decades, landings and post-larval settlement of lobsters in this region, which is near the southern edge of the species' range, have declined substantially, concurrent with a period of significant warming of the coastal waters off southern New England. Previous work has suggested that rising ocean temperatures may adversely impact the survival of larval and early benthic phase (EBP) lobsters, and may cause adult lobsters to seek cooler offshore waters during the critical time of larval release. To investigate the manner in which the observed decline in lobster abundance may be linked to warming coastal waters, a high-resolution hydrodynamic model was used to quantify the increase in water temperature experienced by EBP lobster off SEMA and to supply input to an individual-based model of lobster larval transport from release areas delineated using fishery-dependent data of late-stage egg-bearing lobsters. The results indicate that rising coastal water temperatures may have adversely impacted EBP lobster recruitment off SEMA by (1) causing an offshore shift in the area of larval release that resulted in a reduction in the delivery of larvae to suitable nearshore EBP habitat, and (2) dramatically increasing thermal stress experienced by recently settled EBP lobsters. These findings highlight the implications of warming coastal waters on southern New England lobster population connectivity and provide insight to an understudied mechanism by which climate change affects marine species recruitment.

Keywords

1. Introduction

For coastal communities bordering the Northwest Atlantic Ocean, the American lobster (*Homarus americanus*) holds high ecological, economic, and social value. The American lobster resource off the eastern coast of the United States is currently divided into two biological stock areas: Gulf of Maine/Georges Bank and southern New England (SNE). The latter is situated at the southern edge of the species' coastal distribution (ASMFC, 2020). From the early 1980s to the late 1990s, landings in the SNE stock area increased to reach an all-time high of 9,902 tonnes in 1997 (ASMFC, 2020). While the Gulf of Maine stock to the north continued to grow dramatically after 1997, SNE landings decreased sharply and hit an all-time low of 1,243 tonnes in 2018 (ASMFC, 2020). In concert with this decline in landings, the number of active commercial lobster fishers working in coastal Rhode Island and Massachusetts dropped sharply in the 2000s, by 43% from 1999 to 2011 (Glenn et al., 2011).

This decline in SNE lobster landings is theorized to be a sign of a lobster population stressed by warming waters at the southern edge of its geographic range. Extreme ocean warming played a role in a mass die-off of lobsters in Long Island Sound during the late 1990s (Pearce & Balcom, 2005). Coastal warming has also been implicated in the onset of lethal and persistent epizootic shell disease in the SNE lobster stock, which also began in the late 1990s (Glenn & Pugh, 2006) and has taken a toll on spawning stock, larval settlement and subsequent recruitment to the fishery (Wahle et al., 2009a; Oppenheim et al., 2019). Furthermore, high-resolution monitoring in Rhode Island's Narragansett Bay and offshore coastal waters beginning in 1990 have chronicled a shift of lobster nursery habitat to cooler outer coastal waters (Wahle et al., 2015).

The decline in the SNE lobster stock is reflected in changes in lobster landings and abundance in the NMFS statistical area 538. Situated off southeastern Massachusetts (SEMA) (Figure 1, left panel), area 538 comprises the inshore portion of what was once an extremely profitable inshore commercial fishery, employing approximately 700 commercial lobster fishers in the late 1990s (Glenn et al., 2011). Since 2003, landings from area 538 have remained below the landings recorded over any of the previous 20 years (Figure 2, top panel). Data from fishery-independent trawl surveys conducted off SEMA, over a domain roughly corresponding to area 538 (Figure 1, left panel), by the Massachusetts Division of Marine Fisheries (MADMF) reveal a roughly concurrent decline in spawning stock biomass (*SSB*). The trawl survey data show a drastic reduction in *SSB* during the late 1990s followed by sustained lows, at levels considerably below the *SSB* values recorded in the 1990s, over the next two decades (Figure 2, top panel).

The decline of lobster harvest and *SSB* in area 538 has corresponded with decreasing occurrence of early benthic phase (EBP) juvenile lobsters in the coastal waters off SEMA. The EBP (carapace lengths of 5 – 40 mm; Lawton & Lavalli, 1995) follows the larval planktonic stage when the newly settled lobsters become shelter-restricted and predominantly sedentary (Factor, 1995). The densities of EBP lobsters off the coasts of New England and Atlantic Canada are tracked by the American Lobster Settlement Index (ALSI). Passive bio-collectors (Wahle et al., 2009b) deployed off SEMA in 2009 yielded no EBP lobsters in upper Buzzards Bay (Glenn et al., 2011). In diver-based suction sampling of five Buzzards Bay sites sampled annually from 1998 to 2018, EBP density has remained at or below time series median levels since 2008.

The dramatic lessening of lobster landing, abundance and recruitment observed off SEMA has coincided with an upward trend in sea surface temperatures in the region (e.g. at Woods Hole, MA; Figure 1, right panel). This trend is manifest in the number of degree-days exceeding 19°C (i.e., the sum of amounts by which daily averaged sea surface temperatures exceed 19°C) in a given calendar year (Figure 2, bottom panel). This integrative metric is relevant to lobster distribution in view of the results of controlled laboratory experiments in which adult American lobsters exhibit a preference for water temperatures of 12-18°C and actively avoid temperatures above 19°C (Crossin et al., 1998). The increasing tendency for coastal waters off SEMA to exceed 19°C, particularly in coastal estuaries such as Buzzards Bay, may have played a causal role in the redistribution of late-stage, egg-bearing female lobsters to deeper nearshore waters observed by Glenn et al. (2011). This redistribution of the adult population, coincident with the overall decline in population abundance, may have in turn resulted in a reduction of larval transport to nearshore EBP habitat. Rising coastal temperatures may also have adversely impacted juveniles settled in nearshore habitat as EBP lobsters exhibit a preference for waters in the 13-19°C temperature range (Nielsen & McGaw, 2016).

In view of the temporal correspondence of rising coastal water temperatures with declining abundance of adult and EBP lobsters off SEMA, we put forth the following hypotheses to account for the decline in lobster abundance: (1) the warming of coastal waters beyond the thermal preferences of egg-bearing females resulted in a seaward shift in larval release that has, in turn, depressed larval delivery to coastal settlement habitat off SEMA and (2) the bottom temperatures in that coastal settlement habitat have become overly stressful to EBP lobsters. We tested these hypotheses using a numerical model system comprised of a hydrodynamic model to simulate the currents and thermal regime off SEMA and

an individual-based model (IBM) to account for the transport, growth and mortality of the larval lobster phase. Hypothesis 1 was tested by modeling larval-stage transport between areas of larval release and post-larval settlement. The approach was extended beyond the methodology typically employed in larval-stage transport modeling by developing techniques to delineate areas of larval release and regions with bottom type suitable for post-larval settlement. Hypothesis 2 was tested by defining a metric of thermal stress experienced by EBP lobsters that was evaluated using the hydrodynamic model temperature fields refined with *in situ* temperature data. Through this work, we aimed to improve understanding of the influence of coastal warming on the decline of EBP lobsters off SNE.

2. Methods

2.1 Determination of Larval-Stage Connectivity

To test Hypothesis 1, the probability of larval-stage transport between larval release areas and suitable settlement habitat (referred to hereafter as connectivity) was determined with the following elements:

1. Water velocity and temperature data derived from a regional hydrodynamic model;

2. *In situ* measurements of water temperature used to adjust the model temperatures so that larval growth, which varies as a function of temperature, is most accurately computed;

3. An Individual-Based Model (IBM) of larval growth, mortality and transport; and

4. Specification, based on available data, of areas of larval release for each year considered and of habitat suitable for post-larval lobster settlement.

Details of each element are described below.

The Northeast Coastal Ocean Hydrodynamic Model

Ocean currents and temperature data used as input to the IBM were extracted from archived hindcasts of the Northeast Coastal Ocean Forecasting System (NECOFS) (Beardsley et al., 2013). An integrated atmospheric/ocean/ocean-wave modeling system, NECOFS has a model domain extending from New Jersey to Nova Scotia. The ocean model component, formulated using the Finite-Volume Community Ocean Model (FVCOM) (Chen et al., 2006; Cowles et al., 2008a), has a horizontal grid resolution ranging from 5 km near the open boundary to 500 m along the coast and in the vicinity of persistent tidal mixing fronts. In the vertical, NECOFS's ocean grid consists of 46 layers, which discretize the water column in generalized terrain-following coordinates. The ocean model is driven by a full suite of atmospheric forces (wind stress, heat flux, net precipitation minus evaporation and surface atmospheric pressure) as well as tides, river runoff and water influx into the upstream boundary stretching across the Scotian Shelf.

The performance of the ocean model in the area off southern New England has been evaluated by a number of model-measurement comparison studies. These include tests of model skill in reproducing regional hydrodynamic fields (Cowles et al., 2008b), tidal currents and elevations (Chen et al., 2011), vertical stratification (Li et al., 2015), surface circulation (Sun et al., 2016) and bottom temperatures (Li et al., 2017).

Correcting Model Temperatures

Accurate modeled water temperatures are critical for the calculation of larval growth and for assessing the thermal stress experienced by EBP lobsters. The temperature fields produced by NECOFS are honed by assimilation of daily-averages of sea surface temperature (SST) acquired from satellite-based observations. To avoid gaps due to cloud cover, the SST fields assimilated by NECOFS are spatially

averaged. This produces a bias in the NECOFS temperatures generated in Buzzards Bay, as they are influenced by SST observations in adjacent waters. A result is that model-computed temperatures in the Bay are more reflective of the deeper adjacent waters of Nantucket Sound and exhibit smaller seasonal fluctuations than temperatures observed in the Bay. In the summer and autumn, the time of lobster larval transport, model computed temperatures can be as much as 4°C lower than those measured in the Bay.

As it was important to capture realistic summertime maxima of Buzzards Bay waters for this study, the temperatures within the Bay were adjusted using MADMF bottom temperature measurements at two long-term observation sites: Cleveland Ledge and Bay Mouth (Figure 1). Corrections to model points within the Bay were made at hourly intervals and utilized a spatially varying weight function centered on each observation with a linear decay over a 30 km radius. Corrections were made such that the influence of each MADMF site was directly proportional to the relative distance of model points from either site. For model points up-bay (northeast) of the Cleveland Ledge site, corrections depended solely on deviations between model and *in situ* temperatures at that site and were progressively eased for points farther up-bay to avoid overcorrections.

Simulating Larval Transport, Growth and Mortality

The IBM employed in this study simulated the movement of particles viewed as 'super-individuals', with each representing the growth, mortality and transport of a group of larvae (Scheffer et al., 1995). Larval movement in the horizontal plane was assumed to be passive and was determined by integrating NECOFS velocities, linearly interpolated in space and time, with an explicit fourth-order Runge-Kutta scheme with a time step of 180 s. The influence of sub-grid-scale turbulence was

parameterized using a modified random walk approach (Visser, 1997), which incorporates horizontal

diffusivity scaled to the cell size based on the empirical relationships of Okubo (1971).

After hatching, American lobsters progress through three larval stages (Stage I-III) followed by a

fourth, post-larval, stage (Stage IV) during which they become competent to settle. Field observations

have shown that stage I-III larvae tend to be distributed throughout the ocean's upper mixed layer,

while post-larvae are typically neustonic (Harding et al., 1987). To account for this vertical distribution in

the larval transport simulations, the trajectories of stage I-III larvae were computed using NECOFS

velocities averaged over the upper 5 m, while post-larval trajectories were determined with the near-

surface velocities from NECOFS.

Results of rearing experiments reported by MacKenzie (1988) and Quinn et al. (2013) have

shown that lobster larval development, and the duration of larval stages, is strongly dependent on water

temperature. To account for this dependency in our IBM, the duration of larval stages I-III were

determined from temperature-dependent functions generated by MacKenzie (1988), while the post-

larval stage-IV duration was computed using the temperature-dependent function derived by Incze et al.

(1997) based on MacKenzie's rearing experiment data. We opted for these functions as opposed to

those derived from the data of Quinn et al. (2013) because of the differences in the spatial origins of

lobsters used in the two studies. The lobsters used to produce the larvae used in MacKenzie's

experiments were sourced from more southern areas than those used by Quinn et al., and more likely to

be genetically similar to the lobsters in our study region (see Benestan et al., 2015). We also opted

against applying the reduction factor of larval-stage duration employed by Xue et al. (2008) and Incze et

al. (2010). The factor was based on an analysis of larval samples collected off the Maine coast by Annis

et al. (2007), who proposed that lobster larval development in the wild occurs at roughly twice the rate as that observed by the laboratory studies of MacKenzie (1988). However, Quinn et al. (2013) found that development times from a field study conducted within an isolated archipelago closely matched those of MacKenzie (1988). They argued that the more rapid development rates determined by Annis et al. may be an artifact of including larval cohorts originating at different times and different sites in the calculation of development rate.

The rearing experiments of MacKenzie (1988) also revealed that lobster larval mortality varies with ambient water temperature. This dependency was incorporated in the IBM by fitting the survival data reported by MacKenzie (Table 1 in MacKenzie, 1988) to a quadratic function of survival rate versus temperature for each larval stage.

However, the 10-22°C temperature span of MacKenzie's experiments does not encompass the higher water temperatures observed in our study region during the time when lobster larvae inhabit the water column (June through mid-September). For example, near-bottom (0.5 m above the seafloor) water temperatures recorded at five sites in upper Buzzards Bay during 2012 and 2013 by Hubbard (2016) exceeded 22°C more than 50% of the time over the June through mid-September period.

There is evidence that lobster larval survival may dramatically decrease as temperatures rise above 22°C. The rate of survival to the mid-point of the post-larval stage IV ("S4.5") as derived from MacKenzie's data shows a sharp decrease as water temperatures approach 22°C. The computed survival to S4.5 is 0.74-0.8 in the 14-16°C range and drops to 0.51 at 22°C. It is likely that this trend may continue, or steepen, as temperatures rise above 22°C. Compelling laboratory observations of juvenile

lobster mortality at high temperatures come from the study of Nielsen & McGaw (2016). They report

that EBP lobsters (juvenile stages V-X) die within 30 min when exposed to water at 27°C.

Unfortunately, there are currently no published data available to assign a functional form for

lobster larval mortality between the 22°C upper limit of MacKenzie's experiments and Nielsen &

McGaw's observation of rapid EBP mortality at 27°C. For this study, we opted to fill the 22-27°C gap by

extending the temperature range of the mortality functions derived from MacKenzie's data to a

'breakpoint' of 25.5°C and define mortality as a linear function of temperature from this breakpoint to a

value of 1 (100% mortality) at 27°C. Results obtained from sensitivity studies in which this breakpoint

was varied between 24 and 26°C showed no differences that altered the conclusions of this paper

(Figure S2, Supporting Information).

Daily mortalities determined by MacKenzie's experiments reach a maximum value of 0.13 d^{-1}

(for stage I larvae at 22°C) and tend to be minimal in the 12-18°C range. These laboratory-derived

mortalities do not account for many causes of larval mortality in the wild, particularly due to predation

or food limitation. To account for causes of mortality not included in MacKenzie's study, we have added

a constant 'background mortality' (in addition to the temperature-dependent mortality functions

described above) of 0.2 d^{-1} to the IBM's mortality calculation. This value was employed in lobster larval

transport studies by Chassé & Miller (2010) and Quinn et al. (2017) and is based on analysis of plankton

tow data acquired by Scarratt (1964, 1973). The sensitivity of our results to the choice of background

mortality is considered in the Supporting Information (Figure S1).

Determining the Spatial Distribution of Larval Release and Suitable Juvenile Habitat

Models of larval transport of some species residing in the SNE region have used available data on the spatial dynamics of the species spawning stock in specifying the area of larval release (e.g. Chen et al., 2021). However, prior models of lobster larval transport have predominately targeted connectivity between geographic regions, such as fisheries management areas, without consideration of where in those regions larvae are most likely to be released or to settle as post-larvae (e.g., Incze et al., 2010; Quinn et al., 2017). To more accurately model connectivity, we used available data to delineate the most probable areas of larval release and post-larval settlement.

The specification of post-larval settlement areas was based on studies indicating that post-larvae and EBP lobster preferentially occupy shelter-providing habitat, dominated by cobble-rocks features (Wahle & Steneck, 1991), within a 2-18 m depth range (based on the observations of EBP lobster distribution by Wahle et al., 2013). Data by which cobble-rock areas may be delineated have been acquired by a mapping cooperative between the MA Office of Coastal Zone Management and the US Geological Survey. This cooperative produced more than 1,370,000 measurements of bottom texture within the Massachusetts coastal waters of Buzzards Bay (Figure 3; Foster et al., 2016). The sediment characteristics of each measurement were classified according to a Barnhardt scheme: a 4x4 array with each cell designating the dominant and secondary sediment type (amongst types of rock, gravel, sand and mud; Barnhardt et al., 1998).

Geographically, the settlement area was confined to the Massachusetts coastal waters of Buzzards Bay (Figure 3) for several reasons. Historically, these waters account for the focus of the inshore lobster fishery off SEMA. Both historically and currently, very little active lobstering has occurred in either Vineyard Sound or Nantucket Sound, where the substrate is dominated by sand and is far less

conducive to post-larval settlement. Comprehensive data on sediment characteristics from the mapping cooperative are available in the vicinity of Buzzards Bay. Additionally, the Bay encompasses high-resolution temperature measurements needed to refine the hydrodynamic model's representation of water temperature, and thus thermal suitability for juvenile colonization. Finally, the resolution of the hydrodynamic model degrades for inshore areas west of Buzzards Bay, such as Narragansett Bay, and may not be sufficient for determining post-larval settlement in those areas. Confinement of the settlement area to Buzzards Bay is, nonetheless, appropriate for testing the hypotheses posed in the Introduction as the ALSI data reveal that benthic recruitment to the Bay has exhibited a long-term decline associated with warming waters over the past two decades (detailed below).

As a conservatively strict criterion of settlement suitability, only those measurements from the mapping cooperative with rock as the dominant type were chosen as appropriate settlement habitat. For use in computation of larval transport success, the collection of these measurements was projected onto a 50x50-m cell-size grid encompassing our designated settlement region (Figure 3), with each cell in the depth range of 2-18 m given a value of 1 if it contained a rock-dominated measurement or 0 if it did not.

The larval release area for each year modeled was specified using data from the MADMF commercial sea sampling program (see Estrella & Glenn, 2001) on the location of female lobsters bearing late-stage and spent (recently hatched) eggs. Assuming that these locations corresponded to larval release sites, a protocol was developed to define the boundary containing 95% probability of larval release. First, outliers were identified and excluded using a statistical method known as a "bagplot," or bivariate boxplot (Rousseeuw et al., 1990; Verboven & Hubert, 2010). The kernel density

estimation function 'ksdensity' of MATLAB was applied to the remaining data to produce a probability

density function (PDF) representing the spatial distribution of female lobsters bearing late-stage and

spent eggs. An optimization function was then used to determine a boundary within which 95% of this

probability was contained. For instances in which exceptionally low probability within the boundary was

largely due to the absence of sampling, a minimum probability of 0.002 was imposed. Following this

adjustment, all probability within the original boundary was scaled to return the sum to 0.95. The

portion of the PDF within the 0.95 probability envelope was normalized to integrate to 1. This was then

interpolated to assign each larval release location a discrete release probability (Figure 4).

The larval release area was geographically constricted by the data used to define this area. The

MADMF commercial sea sampling program is principally contained in Massachusetts state territorial

waters, with some exceptions where the lobstering activities of participants exceeds territorial

boundaries (Estrella & Glenn, 2001). Our analysis does not consider the presence of egg-bearing females

in neighboring territorial waters that may potentially contribute to the Buzzards Bay larval supply (e.g.,

from coastal Rhode Island and Connecticut). Furthermore, this application of the commercial fishery-

dependent data comes with the inherent assumption that the commercial lobstering fleet shifts in

accordance with a shift in the bulk of the fished population, and that the observed catch (both landed

and discarded) is thus representative of the adult lobster population. Nevertheless, our approach

provides a data-based method for defining the area of larval release and goes beyond previous

methodology used for determining larval-stage connectivity of a given lobster stock.

To evaluate the role of temperature in limiting the seasonal inshore migrations of egg-bearing

females, the mean (±SD) bottom temperature of the larval release area during the time of larval release

(1 June – 31 July) was determined for each year. The calculations were carried out using daily averaged bottom temperatures from FVCOM refined with *in situ* data as described above. In computing the averages, each model temperature was weighted by the larval release probability in the model cell and by the cell area, as the FVCOM grid is unstructured with uneven cell sizes. Mean bottom temperature of the larval release area was also assessed under a theoretical condition of no offshore shift (since 1991) of the adult female distribution. The non-shifting distribution was set to that derived from 1991 commercial data, as this year had the highest value of *SSB* from spring surveys conducted in the SEMA trawl region and provides a good baseline for evaluating subsequent changes to the fishery.

Computation of Larval Transport Success

Following a number of previous studies (Huret et al., 2007; Churchill et al., 2011, 2017; Lui et al., 2015), connectivity between larval release and settlement locations was represented by the metric of transport success (*TS*). Essentially, this is the probability that a super-individual set out from a release area as defined above (and illustrated in Figure 4) be over settlement-suitable habitat at a settlement-capable development stage. For a single super-individual, *i*, the transport success, TS_i, may be expressed as:

$$TS_i = \frac{\int_{t_1}^{t_2} S_i(\tau)H_i(\tau)d\tau}{t_2-t_1} \tag{1}$$

where τ is the age (time since release) of the super-individual, t_1 age at which the super-individual (as a post-larva) becomes settlement capable, t_2 marks the end of the post-larval stage, $S_i(\tau)$ is the surviving proportion of the original super-individual population at age τ, and $H_i(\tau)$ is a habitat function that equals 1 when the super-individual is over settlement-suitable habitat and is 0 otherwise.

The survival function, S_i, depends both on the background mortality, which is constant over time, and the temperature- and larval-stage-dependent mortality, which varies with time. For a given age, τ, it may be expressed as the product of the fractions of survival over successive time intervals:

$$S_i(\tau) = \prod_{k=0}^{k=\tau/\Delta\tau} [1 - M_B - M_T(k\Delta\tau)] \qquad (2)$$

where M_B is the constant background mortality, M_T is the mortality dependent on temperature and larval stage and $\Delta\tau$ is the time interval over which the survival function is evaluated. M_B and M_T are expressed in units of proportion mortality per unit $\Delta\tau$.

The yearly averaged transport success of super-individuals set out from N sites and over R release times distributed over the larval release season may be expressed as:

$$\overline{TS} = \frac{1}{R}\sum_{k=1}^{R}\sum_{i=1}^{N} P_i TS_{ik} \qquad (3)$$

where TS_{ik} is the transport success of a super-individual released from location i within a release envelope (e.g., Figure 4) and at time k. P_i is the probability of release at point i, and is normalized such that:

$$\sum_{i=1}^{N} P_i = 1 \qquad (4)$$

For each year modeled, $\overline{TS}$ was computed from the equations above using the tracks of super-individuals set out within the year's larval release area, determined as described above. The super-individuals were released from locations spaced 0.75 km apart (Figure 4) and at 6-hr time intervals over

a period extending from 1 June to 31 July. According to analysis of data of late-stage, egg-bearing females acquired over more than 30 years by the MADMF sea sampling program, this period encompasses the time of larval lobster release off SEMA (Glenn et al., 2011).

Based on studies indicating that the settlement behavior of diving and burrowing begins roughly midway through the lobster post-larval stage (Botero & Atema, 1982; Cobb et al., 1989b), the age of settlement capability, t_1, was set at the midpoint of stage IV. The habitat function, H_i, was evaluated using the 50x50-m bottom habitat array described above. The H_i of a settlement-capable super-individual was set to 1 if it resided in a cell designated as a rock-dominant habitat within a depth range of 2-18 m, and was set to 0 otherwise.

The model, parameterized as described above (and summarized in Table 1), was applied for 14 years spanning the period of 1991-2017, which encompasses the sharp decline in lobster abundance off SEMA (Figure 2). The number of years that could be modeled was constrained by limitation of available temperature data (needed to adjust modeled temperatures) and commercial sea sampling data (needed to define the larval release areas). As will be shown, the model results from these years were sufficient to reveal long-terms in larval release area and $\overline{TS}$.

In addition to $\overline{TS}$, the number of post-larvae delivered to settlement-suitable habitat over the course of a year may facilitate an understanding of population connectivity. This may be assumed to be roughly proportional to the product of $\overline{TS}$ and the SSB in the area of larval release, with the assumption that SSB is proportional to the number of larvae released. In computing this product, SSB was estimated using data from the MADMF SEMA trawl surveys (Figures 1 and 2). For each year, SSB was calculated as

the product of the mean weight per tow of fully recruited female lobsters and a locale-specific maturity

curve derived from ova-diameter-adjusted cement-gland data (Estrella & McKiernan, 1989).

2.2 The Thermal Suitability Index

To test Hypothesis 2, a suitability index was developed to assess the thermal stress experienced

by EBP lobsters recently settled off southern Massachusetts. The index was formed from daily averaged

bottom temperatures as determined from the hydrodynamic model temperatures refined with *in situ*

temperature data in the manner described above. For a single model node, i, the annual metric of

thermal suitability, ThS_i, is expressed as:

$$ThS_i = 1 - \frac{dd_i}{dd_{max}} \qquad (5)$$

where dd_i is the number of degree-days above a designated temperature threshold (i.e., the sum of

amounts by which daily averaged bottom temperatures exceed that threshold in a calendar year). The

quantity dd_{max} is the maximum value of dd_i for all model nodes in the designated spatial domain as

determined for the full range of years considered. The threshold temperature of the dd_i calculations was

set at 19°C based on controlled laboratory experiments in which EBP lobsters were allowed to move

freely through a tube with a thermal gradient and exhibited a preference for water temperatures of 13-

19°C, regardless of acclimation temperature or origin (Nielsen & McGaw, 2016).

For a model node in which the temperature is always beneath the threshold during a given year,

the resulting ThS_i of 1 indicates a location with temperatures suitable for juvenile survival. Where dd_i is

equal to dd_{max} (the maximum value of degree-days above the threshold), the resulting ThS_i of 0

indicates a location with the poorest relative thermal suitability. As an additional condition, the thermal

suitability for a node with temperatures reaching or exceeding 27°C at any time in a model year was set to 0 based on the finding that juveniles exposed to such extreme temperatures die within 15-30 minutes (Nielsen & McGaw, 2016).

To evaluate the year-to-year changes in the thermal suitability off SEMA, the yearly averaged thermal suitability, $\overline{ThS}$, of all model nodes, N, within the SEMA settlement region (Figure 3) was determined as:

$$\overline{ThS} = \frac{1}{N} \sum_{i=1}^{N} ThS_i \qquad (6)$$

The above was evaluated for those years over which $\overline{TS}$ was calculated.

2.3 Relating Settlement Index to Water Temperature

The ALSI data combined with the water temperatures recorded at Cleveland Ledge (Figure 1) offer a means to test the relationship of lobster settlement in Buzzards Bay to Bay temperature. While not co-located with any specific ALSI sampling site, the Cleveland Ledge monitor provides a long-term temperature record that is a good representation of the relatively shallow upper Buzzards Bay thermal environment in which most of the ALSI sites reside, especially in the summer when the Bay is very well-mixed. A statistical tendency for settlement to decline with increasing water temperature in the Bay would lend support to both Hypotheses 1 and 2.

As part of the ALSI program, suction surveys were conducted by MADMF at five Buzzards Bay sites over 1998-2018. These sites were selected for their provision of suitable settlement habitat dominated by cobble-rock sediments. The yearly mean EBP density from these surveys shows significant interannual variation combined with a long-term tendency to decline (Figure 5). To evaluate the extent

to which these variations, and decline, in EBP density may be linked to Buzzards Bay's water temperatures, various thermal metrics determined from the Cleveland Ledge temperature record were correlated to EBP density (skewed data transformed using the natural logarithm of density plus a constant of relatively small magnitude).

3. Results

3.1 Year-to-Year Variation in Larval Release Area

The tendency for egg-bearing females to shift seaward over the past three decades is apparent in the PDFs of larval release determined for the selected 14 years of the 1991-2017 time span (Figure 6). With regard to the delivery of larvae to the prescribed post-larval settlement area (Figure 3), two critical properties of this shift are the declining probability of larval release within Buzzards Bay and the tendency of the centroid of the PDF to move offshore and away from the mouth of the Bay.

For modeled years of the 1990s, the majority of larval release probability (~ 82%) originated in Buzzards Bay. By contrast, over the 2000-2007 period, most of the larval release probability (~ 78%) was situated south of and outside the Bay. For 2008-onward, almost all, if not the entirety, of the larval release area was restricted to areas south and seaward of the Bay, with a small release probability (~ 4%) occasionally projecting into the Bay mouth.

The centroids of the larval release probability followed a similar pattern (Figure 6). Over the 1991-2006 period, the centroids spanned the 41.33-41.51 °N latitude band and were situated within or close (< 14 km) to the Bay mouth (as marked by the Bay Mouth temperature station of Figure 1). By

contrast, the centroids of the 2007-2017 period were further south, within the 41.23-41.31 °N latitude band, and ranged from 15 to 25 km from the Bay Mouth temperature station.

The tendency of the larval release area to shift away from warming coastal waters and encompass temperatures suitable for adult females is revealed by comparing the June-July bottom temperature averages within the shifting and the theoretical-stationary release areas. Over the 1990s, mean temperatures determined in the theoretical-stationary (from 1991) and the observed-shifting release areas were comparable, averaging to 16.26°C and 16.11°C, respectively. By contrast, after 2000 the mean temperature of the non-shifting distribution was consistently higher than that of the observed distribution (Figure 7). Over the 2008-2017 period, the June-July mean bottom temperature in the stationary release area averaged to 17.65°C, while the mean temperature of the shifting release area averaged to 14.66°C (Figure 7).

3.2 Year-to-Year Variation in Larval-Stage Connectivity

Corresponding to the long-term seaward trend in larval release area, the yearly averaged transport success ($\overline{TS}$) series shows a clear tendency to decline over the 27-year period of our simulations (Figure 8a; one-tailed Mann-Kendall test, P = 0.0187). The linkage between the decline in $\overline{TS}$ and the offshore shift in release area centroid is most prominent in the 2006-2007 period. The $\overline{TS}$ series exhibits its largest percentage decline going from 2006 to 2007, while the larval release centroid shifts 12.4 km seaward between 2006 and 2007. Beyond this 2-year example, a strong correlation (R^2 = 0.86; P < 0.0001) is exhibited between $\overline{TS}$ and centroid release area latitude (Figure 9), which declines with distance from the Bay mouth except for those 3 centroids within the Bay (Figure 6). Clearly, the delivery

of larvae to the prescribed post-larval settlement zone is highly sensitive to the area of larval release, declining when this release area shifts further offshore.

Although values of $\overline{TS}$ following the 2006-2007 drop are consistently lower than the $\overline{TS}$ values prior to 2006, the $\overline{TS}$ of recent years is trending upward (Figure 8a). However, the product of $\overline{TS}$ times the *SSB* (Figure 8b; one-tailed Mann-Kendall test, P = 0.0244), which takes both connectivity and larval supply into consideration, does not show an increase in recent years. This product has declined over time, with consistently low values (well below the levels of the 1990s) from 2007 onwards. While the *SSB* used in our calculation is from the SEMA trawl region, it is nonetheless indicative of the larger region. *SSB* stock assessment indicators followed similar downward trends throughout SNE during this time. Mean *SSB* from 2007-2018 was below the 25th percentile of the 1981-2018 time series for MA, RI, and CT spring surveys, and below the median in the spring NEFSC survey record (Table 58 in ASMFC, 2020).

3.3 Year-to-Year Variation in the Thermal Suitability Index

The spatially averaged annual thermal suitability, $\overline{ThS}$, for the SEMA settlement region demonstrates a tendency to decline over the 27-year period of our simulations (Figure 8c; one-tailed Mann-Kendall test, P = 0.0008). Between 2000 and 2010, the $\overline{ThS}$ series trends gradually downward and is consistently below the suitability levels determined for model years in the 1990s.

The year-to-year variation and extent of declines in the $\overline{ThS}$ series become more pronounced in the 2010s. Notably, the lowest $\overline{ThS}$ was determined for 2012, a year renowned for extreme summer and autumn ocean temperatures in the Northwest Atlantic Ocean (Mills et al., 2013). In 2012, modeled

bottom temperatures in upper Buzzards Bay reached approximately 26°C, approaching but not meeting

the 27°C limit at which rapid EBP mortality was imposed.

Based on the selection of modeled years, the $\overline{ThS}$ of 2012 and 2016 may initially appear

anomalous in terms of indicating poor thermal suitability in the 2010s. However, calculations of degree-

days exceeding 19°C from *in situ* bottom temperatures at Cleveland Ledge (Figure 5) suggest that the

$\overline{ThS}$ of these years may be characteristic of the recent bottom temperature trends within the Bay, with

the higher $\overline{ThS}$ values of 2014 and 2017 representing anomalies.

3.4 Relation of Settlement Index to Water Temperature

The correlation analysis relating EBP density in Buzzards Bay (as determined from ALSI suction

sampling data) with Bay water temperature (from the Cleveland Ledge temperature record) was

conducted for thermal metrics of days above, and degree-days above, 18, 19, and 20°C. For all metrics,

the EBP/degree-day correlation was negative, indicating a tendency for EBP density to decrease with

warming coastal waters. Degree-days exceeding 19°C had the most significant correlation with natural

log transformed EBP density (Figure 5; Pearson's correlation coefficient, $R = -0.5858$; $P = 0.0084$).

4. Discussion

4.1 Key Findings

Taken together, the results of our analyses indicate that warming coastal waters off SNE

adversely impacted lobster benthic recruitment in a manner consistent with the tested hypotheses: (1) a

seaward shift in larval release due to coastal waters warming beyond the thermal preferences of egg-

bearing females has depressed larval delivery to coastal settlement habitat in Buzzards Bay and (2) the

bottom temperatures in that coastal settlement habitat have become overly stressful to EBP lobsters.

In support of Hypothesis 1 is the long-term decline of yearly averaged transport success ($\overline{TS}$)

coupled with the long-term seaward shift of the estimated larval release area away from the warming

coastal waters within and near Buzzards Bay. The strong linear relationship between the latitude of

release area centroid and $\overline{TS}$ suggests that the variations of $\overline{TS}$ are principally tied to the distance of

larval release from shore, with interannual variations in the regional circulation playing a minor role.

The tendency for the area of larval release to move seaward in concert with rising coastal

temperatures is in line with the MADMF spring trawl survey results, which document the presence of

adult females (carapace lengths of 70+ mm) in Buzzards Bay during the 1980s and 1990s but not in the

2000s and 2010s (MADMF unpublished data). Data from the fishery-independent MADMF ventless trap

survey also reveal a tendency for egg-bearing lobsters to avoid the warmer waters within Buzzards Bay,

with no egg-bearing females in the catch at survey stations in the interior of Buzzards Bay (Pugh &

Glenn, 2020). Bottom temperatures from traps deployed in the shallow survey stratum (<20 m), which

represents most of the survey area within the Bay, were in excess of 19°C for more than 70% of each

year's survey season (Pugh & Glenn, 2020).

Consistent with bottom temperatures observed by Pugh & Glenn (2020), mean June-July bottom

temperatures modeled in our theoretical-stationary larval release area suggest that any egg-bearing

lobsters continuing to make such inshore seasonal migrations would expose themselves to

temperatures approaching and sometimes exceeding the 18°C upper limit of adult preference (Crossin

et al., 1998). The redistribution of egg-bearing lobsters to a thermal environment averaging roughly

three degrees cooler during the time of larval release is well evidenced by a progressively seaward shift in commercial fishing effort. Throughout the 2000s, commercial landings underwent a substantial shift from inshore statistical areas 538 and 539, off the SEMA and Rhode Island coasts, to the more offshore area 537.

Despite the uptick in the latter years of the $\overline{TS}$ time series, severely diminished *SSB* clearly controls the trend of the combined product during these years. This finding suggests that renewed connectivity between the spawning contingent and nursery habitat in Buzzards Bay may not be sufficient for restoring historic levels of benthic recruitment in the Bay.

In support of Hypothesis 2 is the decline of yearly and spatially averaged thermal suitability in the SEMA settlement region. This decline starts gradually in the early 2000s and becomes more pronounced over the last decade. Admittedly, the suitability index is not quantitatively tied to EBP mortality but is based upon thermal preferences exhibited by both EBP lobsters and larger sub-adults as reported in the literature (Crossin et al., 1998; Nielsen & McGaw, 2016). Nevertheless, the trend of this index suggests that EBP lobsters settled off SEMA have encountered an increasingly stressful environment over the past two decades. If mortality is indeed linked to the thermal suitability index, then the mortality associated with the particularly low values of the index observed since 2010 may effectively stymie a recovery of the lobster population off SEMA following the abrupt decline in abundance observed in the early 2000s (ASMFC, 2020).

The combination of our findings with the observations of Pugh & Glenn (2020) suggests that the tendency of EBP lobster density off SEMA to decline with degree-days above 19°C may be ascribed to two factors: the seaward retreat of egg-bearing lobsters from warming coastal waters and the thermal

stress experienced by EBP lobsters when exposed to prolonged periods of water temperatures above 19°C. The negative influence of these two factors on benthic recruitment is exacerbated by the extremely low abundance of reproductive adults. The multiple factors contributing to low adult abundance in SNE are either caused by or intensified by the changing thermal habitat. These factors include increases in natural mortality due to disease (Shields 2013; 2019) and predation (Le Bris et al., 2018), as well as decreases in lobster fecundity (Goldstein et al., 2022).

4.2 Model Limitations

This study necessarily relies on assumptions regarding lobster distribution and various aspects of egg hatching and larval biology. With regard to delineating the area of larval release, the MADMF commercial lobster sampling provides the best available dataset for identifying the spatial locations of ovigerous females at or near the time of hatching. However, as noted in the Methods, there are issues with the extent to which these data represent the true distribution of egg-bearing females. The MADMF sea sampling program has varied over space and time. Since the mid-2000s, an offshore shift in the fishing effort has prompted a corresponding shift in the sampling, with more sampling trips being carried out statistical area 537, which is offshore of area 538. In addition, the total number of annual sampling trips has also declined somewhat due to logistical challenges (MADMF unpublished data). While these changes in sampling may have impacted the ability to consistently track the locations of ovigerous females, the offshore shift observed in the sea sampling data is substantiated by the fishery-independent datasets from the MADMF spring trawl survey and the MADMF ventless lobster trap survey, both of which show an absence of reproductive females in upper Buzzards Bay sampling stations since the 2000s (Section 4.1). Furthermore, station-specific catch data from the ventless trap survey

show that total catch (all lobsters) in the interior stations was consistently much lower than catch in stations near the mouth of the Bay in deeper waters, a further indication that the interior of the Bay is not currently viable lobster habitat (Pugh and Glenn, 2020). Finally, a spatial modeling analysis presented in the 2020 lobster stock assessment, based on Federal and state trawl survey data, reveals an offshore shift and overall decline in SNE lobster population density, with the density within Buzzards Bay and many inshore areas declining over time (Figure 41 in ASMFC, 2020). Thus, while the commercial trap sampling dataset isn't without bias, the offshore shift it shows is consistent with other datasets.

Unfortunately, the time of the trawl surveys does not coincide with the time of lobster egg hatch, making the catch data from the surveys less than ideal for representing larval release locations. Future applications of our methodology for defining larval connectivity would benefit from more representative sampling of the target population(s) to better characterize the distribution of egg-bearing lobsters at the time of egg hatch.

Another assumption inherent in model parameterization is the time-invariant larval release period extending from 1 June to 31 July. While this period encompasses the bulk of hatch observed over more than 30 years of commercial sampling off SEMA, data occasionally show evidence of hatching (spent eggs) during the month of May (MADMF unpublished data). This variability in the observed timing of hatch may be partly due to differences in the timing of sampling trips during the month of May as well as actual year-to-year variation in hatch timing, the latter being likely temperature-driven. Future modeling work would benefit from an examination of connectivity and survival under differing scenarios of hatch timing, both in terms of a shift in timing and in terms of a broadening of the hatch time period.

Horizontal movement in the larval transport model was assumed to be passive for all stages, despite studies demonstrating that post-larvae exhibit directional swimming (Cobb et al., 1989a) that may impact dispersal potential (Katz et al., 1994). We chose to assume strictly passive post-larval movement, which was the assumption imposed in earlier larval lobster IBMs (Xue et al., 2008; Incze et al., 2010; Chassé & Miller, 2010; Quinn et al., 2017), due to the absence of sufficient data needed to model post-larval swimming behavior.

Perhaps most importantly, our conclusions are limited by the current lack of information on the effects of high ambient temperatures on the survival of larval and EBP lobsters. While the experiments of Nielsen & McGaw (2016) suggest that EBP lobsters prefer temperatures below 19°C and experience rapid mortality at 27°C, the lobsters from their experiments were sourced from regions of cooler water than found off SEMA. Despite varying acclimation temperatures utilized prior to their experiments, it is possible that the influence of local adaptation persists in the lobster's response to temperature thresholds. Accounting for EBP mortality in the broad temperature range between 19 and 27°C requires information not currently available. To better quantify the effect of rising coastal water temperatures on lobster benthic recruitment, we recommend that studies be conducted to determine the mortality of larval and EBP lobsters at high water temperatures not currently accounted for in laboratory studies but frequently observed in the waters off SNE.

4.3 Conclusions and Broader Application

Rising coastal water temperatures have broad implications for virtually all life stages of American lobster. Focusing on a particularly data-rich sub-region of the SNE stock domain, we have documented how rising coastal water temperatures may threaten sustained larval connectivity between

a dwindling spawning contingent and historically utilized nursery habitat. The study of climate warming's influence on recruitment failure occurring in the larval stages has often emphasized the role of temporal mismatches between larval production and food supply or favorable winds (Cushing, 1974; 1990; Durant et al., 2007). The finding that diminishing benthic settlement may occur in response to a seaward retreat in larval release locations offers an example of an understudied mechanism by which climate change may affect fishery recruitment.

The shift in lobster landings from inshore to offshore statistical areas was reflected throughout SNE, historically an inshore-dominated fishery (ASMFC, 2020). Recent studies (Mazur et al., 2020; Tanaka et al., 2020) have linked an offshore shift in adult lobster abundance to a loss of viable inshore adult habitat due to changing environmental conditions, including rising temperatures. By exploring the consequence of environmental change on settlement and thermal suitability in historical nursery habitat for early life stages, we have sought to more wholly consider the impacts of coastal warming on lobster benthic recruitment.

Fishery-independent ventless trap surveys conducted in SNE have recently documented practically zero abundance of successive juvenile stages (carapace lengths of 53+ mm) in estuaries including Buzzards Bay and Narragansett Bay (McManus et al., 2021). Severely diminished *SSB* in SNE makes recovery of the fishery highly unlikely. Moreover, the relatively high temperatures currently observed in the waters off SNE are likely to become common over an increasing expanse of the American lobster's ecological range as coastal waters warm (Rheuben et al., 2017). Thus, this case study contributes to a broader understanding of the role of coastal warming in lobster recruitment in SNE and beyond.

References

Annis, E. R., Incze, L. S., Wolff, N., and Steneck, R. S. (2007). Estimates of *in situ* larval development time for the lobster, *Homarus americanus*. *Journal of Crustacean Biology*, 27, 454-462.

Atlantic States Marine Fisheries Commission (ASMFC) (2020). 2020 American lobster benchmark stock assessment and peer review report. National Oceanic and Atmospheric Administration. Atlantic States Marine Fisheries Commission. Boston, MA.

Barnhardt, W. A., Kelley, J. T., Dickson, S. M., & Belknap, D.F. (1998). Mapping the Gulf of Maine with side-scan sonar: A new bottom-type classification for complex seafloors. *Journal of Coastal Research*, 14, 646-659.

Beardsley, R. C., Chen, C., & Xu, Q. (2013). Coastal flooding in Scituate (MA): a FVCOM study of the 27 December 2010 nor'easter. *Journal of Geophysical Research, Oceans*, 118, 6030–6045. https://doi.org/10.1002/2013JC008862

Benestan, L., Gosselin, T., Perrier, C., Sainte-Marie, B., Rochette, R., & Bernatchez, L. (2015). RAD genotyping reveals fine-scale genetic structuring and provides powerful population assignment in a widely distributed marine species, the American lobster (*Homarus americanus*). *Molecular Ecology*, 24, 3299-3315. https://doi.org/10.1111/mec.13245

Botero, L., & Atema, J. (1982). Behavior and substrate selection during larval settling in the lobster *Homarus americanus*. *Journal of Crustacean Biology*, 2, 59-69.

Chassé, J., & Miller, R. J. (2010). Lobster larval transport in the southern Gulf of St. Lawrence. *Fisheries Oceanography*, 19, 319-338.

Chen, C., Huang, H., Beardsley, R. C., Xu, Q., Limeburner, R., Cowles, G. W., Sun, Y., Qi, J., & Lin, H. (2011). Tidal Dynamics in the Gulf of Maine and New England Shelf: An Application of FVCOM. *Journal of Geophysical Research*, 116. https://doi.org/10.1029/2011JC007054

Chen, C., Zhao, L., Gallager, S., Ji, R., He, P., Davis, C., Beardsley, R.C., Hart, D., Gentleman, W.C., Wang, L., Li, S., Lin, H., Stokesbury, K., Bethoney, D. (2021). Impact of larval behaviors on dispersal and connectivity of sea scallop larvae over the northeast U.S. shelf. *Progress in Oceanography*, 195.

Chen, C., Beardsley, R. C., & Cowles, G.W. (2006). An unstructured grid, finite-volume coastal ocean model (FVCOM) system. *Oceanography*, 19, 78–89. https://doi.org/10.5670/oceanog.2006.92

Churchill, J. H., Kritzer, J. P., Dean, M. J., Grabowski, J. H., & Sherwood, G. D. (2017). Patterns of larval stage connectivity of Atlantic cod (*Gadus morhua*) within the Gulf of Maine in relation to current structure and a proposed fisheries closure. *ICES Journal of Marine Science*, 74, 20-30.

Churchill, J. H., Runge, J., & Chen, C. (2011). Processes controlling retention of spring-spawned Atlantic cod *(Gadus morhua*) in the western Gulf of Maine and their relationship to an index of recruitment success. *Fisheries Oceanography*, 20, 32-46.

Cobb, J. S., Wang, D., Campbell, D. B., & Rooney, P. (1989a). Speed and direction of swimming by postlarvae of the American lobster. *Transactions of the American Fisheries Society*, 118, 82-86.

Cobb, J. S., Wang, D., & Campbell, D. B. (1989b). Timing of settlement by postlarval lobsters (*Homarus americanus*): Field and laboratory evidence. *Journal of Crustacean Biology*, 9, 60-66.

Cowles, G. W. (2008a). Parallelization of the FVCOM Coastal Ocean Model. *International Journal of High Performance Computing Applications*, 22, 177–193.

Cowles, G. W., Lentz, S. J., Chen, C., Xu, Q., & Beardsley, R. C. (2008b). Comparison of observed and model-computed low frequency circulation and hydrography on the New England Shelf. *Journal of Geophysical Research, Oceans*, C09015. https://doi.org/10.1029/2007JC004394

Crossin, G. T., Al-Ayoub, S .A., Jury, S. H., Howell, W. H., & Watson, W. H. III (1998). Behavioral thermoregulation in the American lobster *Homarus americanus*. *Journal of Experimental Biology* 201, 365-374.

Cushing, D. H. (1974). The natural regulation of fish populations. In: Harden-Jones, F. R. (ed) Sea fisheries research. *Elek Science*, London, 399-412.

Cushing, D. H. (1990). Plankton production and year-class strength in fish populations: An update of the match/mismatch hypothesis. *Advances in Marine Biology*, 26, 249-293.

Durant, J. M., Hjermann, D. Ø., Ottersen, G., & Stenseth, N. C. (2007). Climate and the match or mismatch between predator requirements and resource availability. *Climate Research*, 33, 271-283.

Estrella, B. T. & Glenn R. P. (2001). Massachusetts Coastal Commercial Lobster Trap Sampling Program May—November, 2000. Massachusetts Division of Marine Fisheries Technical Report TR-7, 21 pp.

Estrella, B. T. & McKiernan, D. J. (1989). Catch-per-unit-effort and biological parameters from the Massachusetts coastal lobster (*Homarus americanus*) resource: Description and trends. NOAA Technical Report NMFS 81, 21 pp.

Factor, J. R. (1995). Introduction, anatomy, and life history. In: Factor, J.R. (ed) Biology of the lobster *Homarus americanus*. *Academic Press*, San Diego, CA, 1-11.

Foster, D. S., Baldwin, W. E., Barnhardt, W. A., Schwab, W. C., Ackerman, S. D., Andrews, B. D., & Pendleton, E.A. (2016). Shallow geology, sea-floor texture, and physiographic zones of Buzzards Bay, Massachusetts (ver. 1.1, June 2016): U.S. Geological Survey Open-File Report 2014–1220. https://dx.doi.org/10.3133/ofr20141220

Glenn, R.P. & Pugh, T.L. (2006). Epizootic shell disease in American lobster (*Homarus americanus*) in Massachusetts coastal waters: Interactions of temperature, maturity, and intermolt duration. *Journal of Crustacean Biology*, 26, 639-645.

Glenn, R. P., Pugh, T. L., Manning, J., Gibson, M., Dellinger, L., Angell, T., DeCosta, A., Wahle, R.A., & Wilcox, S. (2011). Examining settlement dynamics of postlarval American lobster, *Homarus americanus*, in Lobster Management Area 2. Final Report, Part I, Southern New England Collaborative Research Initiative, NOAA Grant Number NA08NMF4720595, 77 pp.

Goldstein, J. S., Zarrella-Smith, K. A., & Pugh, T. P. (2022). Recent declines in American lobster fecundity in southern New England: drivers and implications. *ICES Journal of Marine Science*, 2022, 1-13. https://doi.org/10.1093/icesjms/fsac083

Harding, G. C., Pringle, J. D., Vass, W. P., Pearre, S. J., & Smith, S. J. (1987). Vertical distribution and daily movements of larval lobsters *Homarus americanus* over Browns Bank, Nova Scotia. *Marine Ecology Progress Series*, 41, 29-41.

Hubbard, W. A. (2016). Benthic studies in upper Buzzards Bay, Massachusetts: 2011/12 as compared to 1955. *Marine Ecology*, 37, 532-542. 37.10.1111/maec.12275.

Huret M., Runge J. A., Chen C., Cowles G. W., Xu Q., & Pringle J. M. (2007). Dispersal modeling of fish early life stages: sensitivity with application to Atlantic cod in the western Gulf of Maine. *Marine Ecology Progress Series*, 347, 261–274.

Incze, L. S., Wahle, R. A., & Cobb, J. S. (1997). Quantitative relationships between postlarval production and benthic recruitment in lobsters, *Homarus americanus*. *Marine Freshwater Research*, 48, 729–743.

Incze, L. S., Xue, H., Wolff, N., Xu, D., Wilson, C., Steneck, R., Wahle, R. A., Lawton, P., Pettigrew, N., & Chen, Y (2010). Connectivity of lobster (*Homarus americanus*) populations in the coastal Gulf of Maine: Part II. coupled biophysical dynamics. *Fisheries Oceanography*, 19, 1-20.

Katz, C.H., Cobb, J.S., & Spaulding, M. (1994). Larval behavior, hydrodynamic transport, and potential offshore-to-inshore recruitment in the American lobster *Homarus americanus*. *Marine Ecology Progress Series*, 103(3), 265-273.

Lawton, P., & Lavalli, K. (1995). Postlarval, juvenile, adolescent, and adult ecology. In: Factor, J.R. (ed) Biology of the lobster *Homarus americanus*. *Academic Press*, San Diego, CA, 47-88.

Le Bris, A., Mills, K. E., Wahle, R. A., Chen, Y., Alexander, M. A., Allyn, J. A., Schuetz, J. G., Scott, J. D., & Pershing, A. J. (2018). Climate vulnerability and resilience in the most valuable North American fishery. *Proceedings of the National Academy of Sciences*, 115, 1831-1836.

Li, B., Tanaka, K. R., Chen, Y., Brady, D. C., & Thomas, A. C. (2017). Assessing the quality of bottom water temperatures from the Finite-Volume Community Ocean Model (FVCOM) in the Northwest Atlantic Shelf region. Journal of Marine Systems, 173, 21-30. https://doi.org/10. 1016/j.jmarsys.2017.04.001

Li, Y., Fratantoni, P. S., Chen, C., Hare, J. A., Sun, Y., Beardsley, R. C., & Ji, R. (2015). Spatio-temporal patterns of stratification on the Northwest Atlantic shelf. *Progress in Oceanography*, 134, 123-137. http://dx.doi.org/10.1016/j.pocean.2015.01.003

Liu, C., Cowles, G. W., Churchill, J. H., & Stokesbury, K. D. E. (2015). Connectivity of the bay scallop (*Argopecten irradians*) in Buzzards Bay, Massachusetts, U.S.A. *Fisheries Oceanography*, 24, 364-382

MacKenzie, B. R. (1988). Assessment of temperature effects on interrelationships between stage durations, mortality, and growth in laboratory-reared *Homarus americanus* Milne Edwards larvae. *Journal of Experimental Marine Biology and Ecology*, 116, 87-98.

Mazur, M. D., Friedland, K. D., McManus, M. C., & Goode, A. G. (2020). Dynamic changes in American lobster suitable habitat distribution on the Northeast U.S. Shelf linked to oceanographic conditions. *Fisheries Oceanography*, 29, 349-365.

McManus, M. C., Kipp, J., Shank, B., Reardon, K., Pugh, T. L., Carloni, J., & McKown, K. (2021). A model-based approach to standardizing American lobster (*Homarus americanus*) ventless trap abundance indices. *Fisheries Research*, 238.

Mills, K. E., Pershing, A. J., Brown, C. J., Chen, Y., Chiang, F. S., Holland, D. S., Lehuta, S., Nye, J. A., Sun, J. C., Thomas, A. C., & Wahle, R. A. (2013). Fisheries management in a changing climate: Lessons from the 2012 ocean heat wave in the Northwest Atlantic. *Oceanography*, 26, 191–195. https://doi.org/10.5670/oceanog.2013.27

Nielsen, T. V. & McGaw, I. J. (2016). Behavioral thermoregulation and trade-offs in juvenile lobster *Homarus americanus*. *The Biological Bulletin*, 230, 35-50.

Okubo, A. (1971). Oceanic diffusion diagrams. *Deep-Sea Research*, 18, 789-802.

Oppenheim, N., Wahle, R. A., Brady, D. C., Goode, A. G., & Pershing, A. J. (2019). The cresting wave: Larval settlement and ocean temperatures predict change in the American lobster harvest. *Ecological Applications*, 29. https://doi.org/10.1002/eap.2006

Pearce, J. & Balcom, N. (2005). The 1999 Long Island Sound lobster mortality event: Findings of the comprehensive research initiative. *Journal of Shellfish Research*, 24, 691-697. https://doi.org/10.2983/0730-8000(2005)24[691:TLISLM]2.0.CO;2

Pugh, T. L. & Glenn, R. P. (2020). Random stratified ventless trap survey for American lobster 2006-2016. MADMF Technical Report TR-71, 63 pp.

Quinn, B. K., Chasse, J., & Rochette, R. (2017). Potential connectivity among American lobster fisheries as a result of larval drift across the species' range in eastern North America. *Canadian Journal of Fisheries and Aquatic Sciences*, 74, 1549-1563.

Quinn, B. K., Rochette, R., Ouellet, P., & Sainte-Marie, B. (2013). Effect of temperature on development rate of larvae from cold-water American lobster (*Homarus americanus). Journal of Crustacean Biology*, 33, 527-536.

Rheuben, J. E., Kavanaugh, M. T., & Doney, S. C. (2017). Implications of Future Northwest Atlantic Bottom Temperatures on the American Lobster (*Homarus americanus*) Fishery*, Journal of Geophysical Research, Oceans*, 122, 9387-9398.

Rousseeuw, P. J., Ruts, I., & Tukey, J. W. (1990). The bagplot: A bivariate boxplot. *The American Statistician*, 53, 87-88.

Scarratt, D.J. (1973). Abundance, survival, and vertical and diurnal distribution of lobster larvae in

Northumberland strait, 1962-1963, and their relationships with commercial stocks. J Fish Res Bd

Can 24:1819-1824.

Scarratt, D. J. (1964). Abundance and distribution of lobster larvae (*Homarus americanus*) in

Northumberland Strait. *Journal of the Fisheries Research Board of Canada*, 21, 661–680.

Scheffer, M., Baveco, J. M., DeAngelis, D. L, Rose, K. A., & van Nes, E. H. (1995). Super-individuals a

simple solution for modelling large populations on an individual basis. *Ecological Modeling*, 80, 161-

170.

Shields, J. D. (2013). Complex etiologies of emerging diseases in lobsters (*Homarus americanus*) from

Long Island Sound. *Canadian Journal of Fisheries and Aquatic Sciences*, 70, 1576-1587.

Shields, J. D. (2019). Climate change enhances disease processes in crustaceans: case studies in lobsters,

crabs, and shrimps. *Journal of Crustacean Biology*, 39, 673-683.

Sun, Y., Chen, C., Beardsley, R. C., Ullman, D., Butman, B., & Lin, H. (2016). Surface circulation in Block

Island Sound and adjacent coastal and shelf regions: A FVCOM-CODAR comparison. *Progress in

Oceanography*, 143, 26-45. https://doi.org/10.1016/j.pocean.2016.02.005

Tanaka, K. R., Torre, M. P., Saba, V. S., Stock, C. A., & Chen, Y. (2020). An ensemble high-resolution

projection of changes in the future habitat of American lobster and sea scallop in the Northeast US

continental shelf. *Diversity and Distributions*, 26, 987-1001.

Verboven, S., & Hubert, M. (2010). MATLAB library LIBRA. *Wiley Interdisciplinary Review of

Computational Statistics*, 2, 509-515.

Visser, A. (1997). Using random walk models to simulate the vertical distribution of particles in a turbulent water column. *Marine Ecology Progress Series*, 158, 275–281.

Wahle, R. A., Bergeron, C., Tremblay, J., Wilson, C., Burdett-Coutts, V, Comeau, M., Rochette, R., Lawton, P., Glenn, R. P., & Gibson, M. (2013). The geography and bathymetry of American lobster benthic recruitment as measured by diver-based suction sampling and passive collectors, *Marine Biology Research*, 9, 42-58.

Wahle, R. A., Dellinger, L., Olszewski, S., & Jekielek, P. (2015). American lobster nurseries of southern New England receding in the face of climate change. *ICES Journal of Marine Science*, 72, i69-i78. https://doi.org/10.1093/icesjms/fsv093

Wahle, R. A., Gibson, M., & Fogarty, M. J. (2009a). Distinguishing disease impacts from larval supply effects in a lobster fishery collapse. *Marine Ecology Progress Series*, 376, 185-192. https://doi.org/10.3354/meps07803

Wahle, R. A., Wilson, C., Parkhurst, M., and Bergeron, C. E. (2009b). A vessel-deployed passive postlarval collector to assess settlement of the American lobster *Homarus americanus*. *New Zealand Journal of Marine and Freshwater Research*, 43, 465-474.

Wahle, R. A. and Steneck, R. (1991). Recruitment habitats and nursery grounds of the American lobster Homarus americanus: A demographic bottleneck? *Marine Ecology Progress Series*, 69, 231-243.

Xue, H., Incze, L., Xu, D., Wolff, N., and Pettigrew, N. (2008). Connectivity of lobster populations in the coastal Gulf of Maine - Part I: Circulation and larval transport potential. *Ecological Modeling*, 210, 193-211.

Tables

Table 1 – Methods and parameters applied in the Individual-Based Model

Parameter	Stages	Method/Parameter (T is temperature)	Source
Advection	I-III	Integration of velocities averaged over 0-5 m	Harding et al. (1987)
Advection	IV	Integration of surface velocities	Harding et al. (1987)
Growth	I-III	$D = 851(T-0.84)^{-1.91}$ Duration Stage I $D = 200(T-4.88)^{-1.47}$ Duration Stage II $D = 252(T-5.30)^{-1.45}$ Duration Stage III	MacKenzie (1988)
Growth	IV	$D = 703.49T^{-1.2569}$ Duration Stage IV	Incze et al. (1997) based on MacKenzie's data
Mortality: T-dependent	I-IV	Stage-dependent quadratic function of T (based on laboratory data) to 25.5°C, and a linear function of T to extinction at 27°C	MacKenzie (1988) Nielsen & McGaw (2016)
Mortality: Background	I-IV	0.2 d^{-1}	Chassé & Miller (2010) using data & analysis from Scarratt (1964, 1973)
Settlement Capability	IV	Post-larvae become settlement capable halfway through stage IV	Botero & Atema (1982) Cobb et al. (1989b)
Settlement Area	IV	2-18 m depth with rock-dominated habitat	Wahle & Steneck (1991) Wahle et al. (2013)
Larval Release Area		Determined from distribution of spent & late-stage female lobsters	MADMF commercial sea sampling program

Figure captions

Figure 1. Left panel: Southeastern Massachusetts (SEMA) coastline with the location of NMFS statistical area 538 (data source: NOAA Northeast Fisheries Science Center, ftp://ftp.nefsc.noaa.gov/pub/gis/), as well as the SEMA region of bottom trawl surveys conducted by MADMF (data source: MADMF). Right panel: Enhanced view of Buzzards Bay with locations of three stations with long-term water

temperature observations. The Bay mouth and Cleveland Ledge stations are operated by MADMF and record bottom temperature. The Woods Hole station, currently operated by NOAA's National Ocean Service, records sea surface temperature.

Figure 2. Top panel: Commercial lobster landings from NMFS statistical area 538 (bars) and spawning stock biomass (*SSB*) estimated from spring bottom trawl surveys conducted by MADMF in the SEMA region (dotted line) (data source: MADMF). Bottom panel: Annual deviations from the time series mean number of degree-days above 19°C calculated from sea surface temperatures recorded at Woods Hole, MA (2012 data unavailable; data sources: NOAA National Data Buoy Center, https://www.ndbc.noaa.gov/station_page.php?station=bzbm3 and Woods Hole Oceanographic Institution Data Library and Archives, http://dlaweb.whoi.edu/water_temperatures/water_temp.php). The degree-days value for each year represents the sum of amounts by which daily averages exceeded 19°C. The time series mean is 218 degree-days.

Figure 3. In computing transport success, post-larval lobster settlement was restricted to locations in Buzzards Bay with depths between 2 and 18 meters and with surficial sediments dominated by rock. The Buzzards Bay settlement domain polygon, 18-meter isobath, and rock-dominant classification are shown (surficial sediments data source: Massachusetts Ocean Resource Information System, http://maps.massgis.state.ma.us/map_ol/moris.php; see Foster et al., 2016). Also shown are the locations of five suction sites sampled annually as part of the ALSI monitoring program.

Figure 4. Modeled larval release probability applied to distinct release locations for an example model year (1991). Release probability has been interpolated from a probability density function (PDF) characterizing the spatial distribution of late-stage and spent egg-bearing lobsters in commercial sampling data collected by MADMF. The release boundary (solid black line) was determined as the boundary containing the uppermost 95% of this original probability.

Figure 5. Top panel shows density (individuals per m^2) of EBP lobsters from suction surveys conducted at five ALSI sites in Buzzards Bay (bars; data source: MADMF; 2015-2017 indicate zero density) and number of degree-days above 19°C calculated from bottom temperatures recorded at Cleveland Ledge (dotted line; data source: MADMF; 2004-2005 not included due to an incomplete temperature record). Bottom panel shows natural log transformed EBP density from the five sites plotted against the number of degree-days above 19°C at Cleveland Ledge, with least squares regression shown (dashed line; 2004 and 2005 not included in regression or correlation). Pearson's correlation coefficient, $r = -0.5858$; $P = 0.0084$.
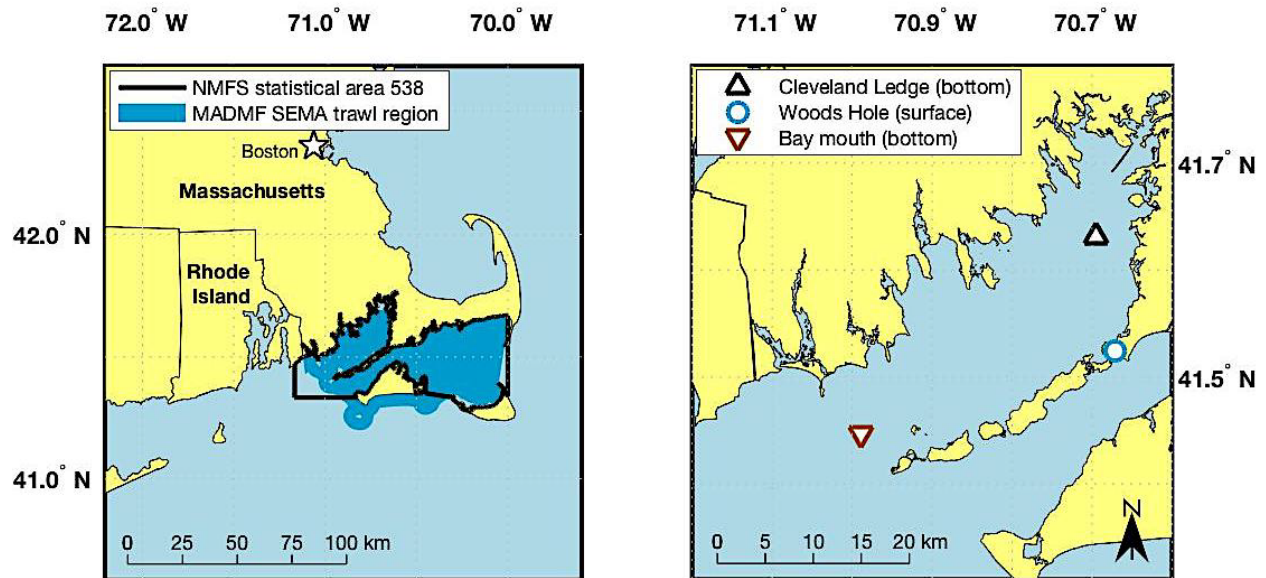
Figure 6. Mean June 1 – July 31 bottom temperature from GOM-FVCOM model configuration refined with *in situ* temperature data. The probability-weighted average temperature over larval release areas (black boundaries) is denoted by $\bar{T}_{eggers}$. The centroid of the larval release probability within each release area is marked by a black dot.

Figure 7. Mean (± SD) June 1 – July 31 bottom temperatures for an offshore-shifting distribution of egg-bearing female lobsters (observed condition) and a non-shifting distribution (theoretical condition; 1991 boundary assumed for all years). The error bars represent the spatial standard deviation in average June-July temperatures.
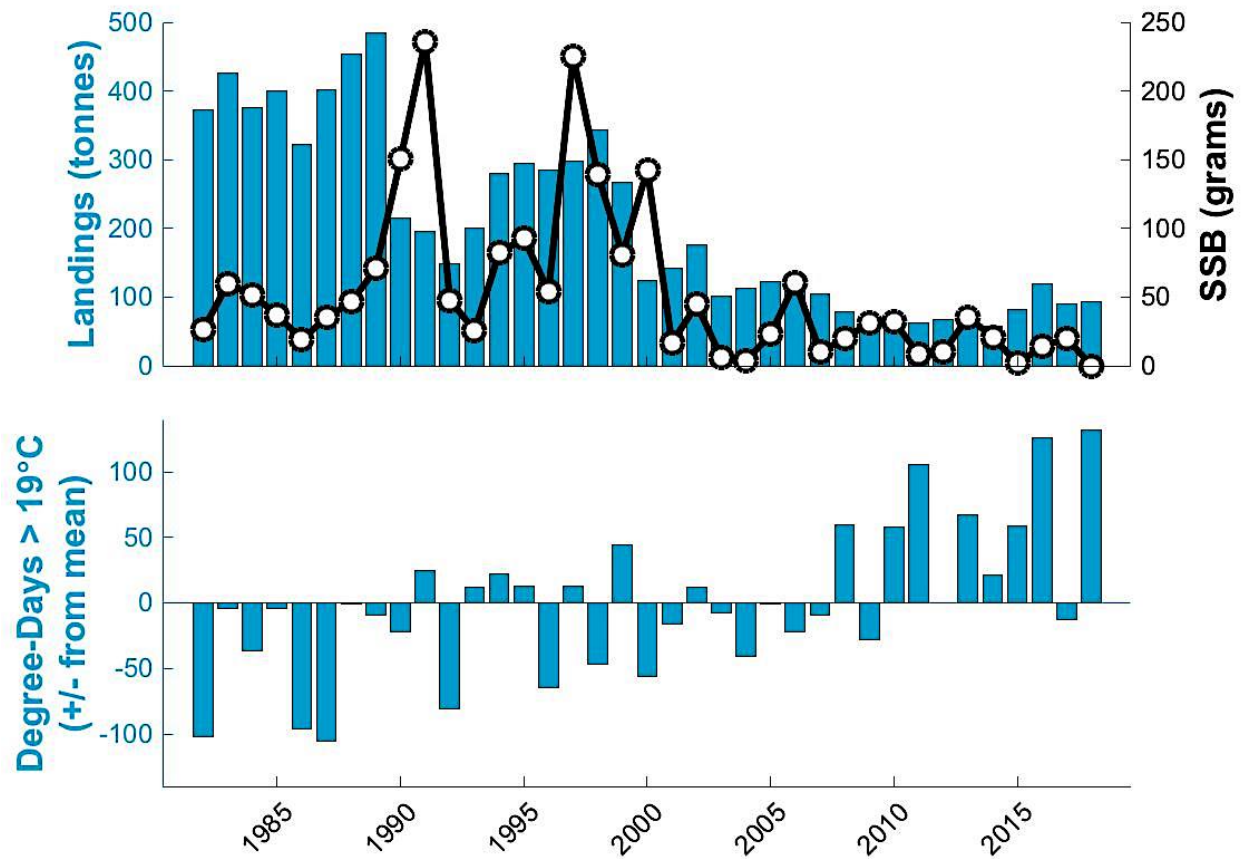
Figure 8. Summary, in the form of spatial and yearly averages, of the transport success and thermal suitability calculations: (a) yearly averaged transport success ($\overline{TS}$), (b) $\overline{TS}$ x *SSB*, where spawning stock biomass (*SSB*) is assumed to be proportional to the overall supply of larvae released in the SNE region, and (c) yearly and spatially averaged thermal suitability index ($\overline{ThS}$). One-tailed Mann-Kendall tests confirmed significant downward trends: P(a) = 0.0187; P(b) = 0.0244; P(c) = 0.0008. Taken together, the trends indicate degrading probability of larval transport to the designated settlement area (Figure 3) and degrading thermal suitability for EBP survival within that area.

Figure 9. The yearly averaged transport success ($\overline{TS}$) plotted against the latitude of the centroid of the larval release probability of each year (Figure 6). $\overline{TS}$ is strongly correlated (R^2 = 0.86; P< 0.0001) with the centroid latitude (which roughly decreases with distance from shore) implying that the delivery of larvae to near-shore habitat suitable for juvenile settlement declines as the area of larval release shifts offshore.
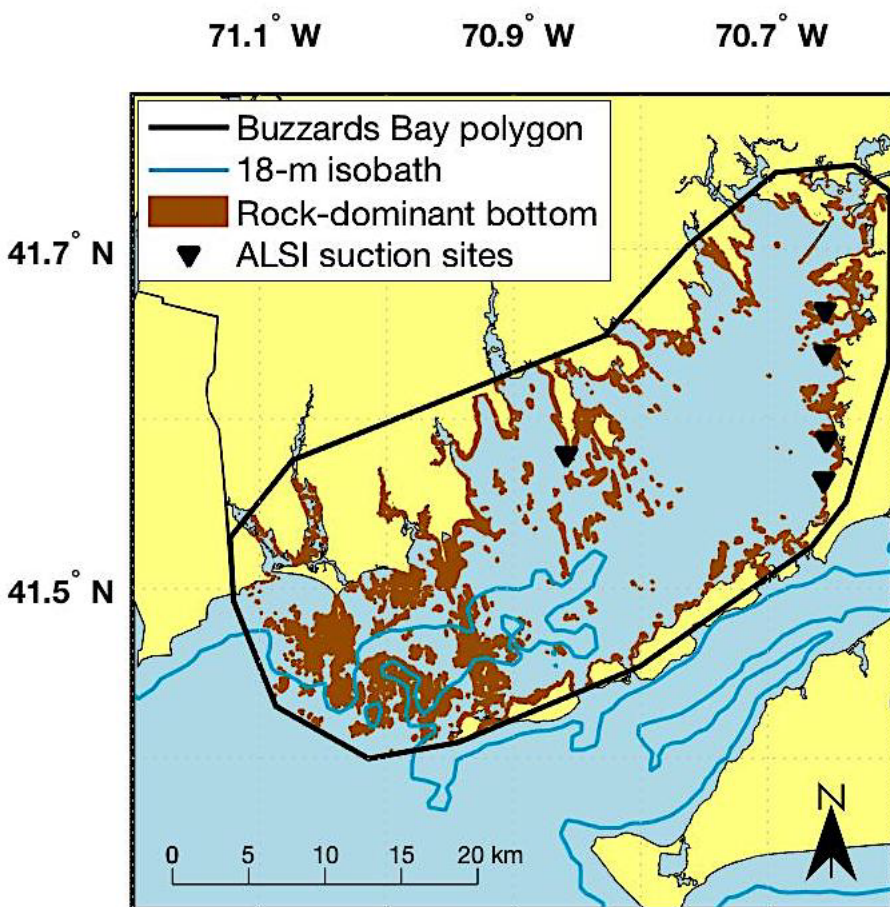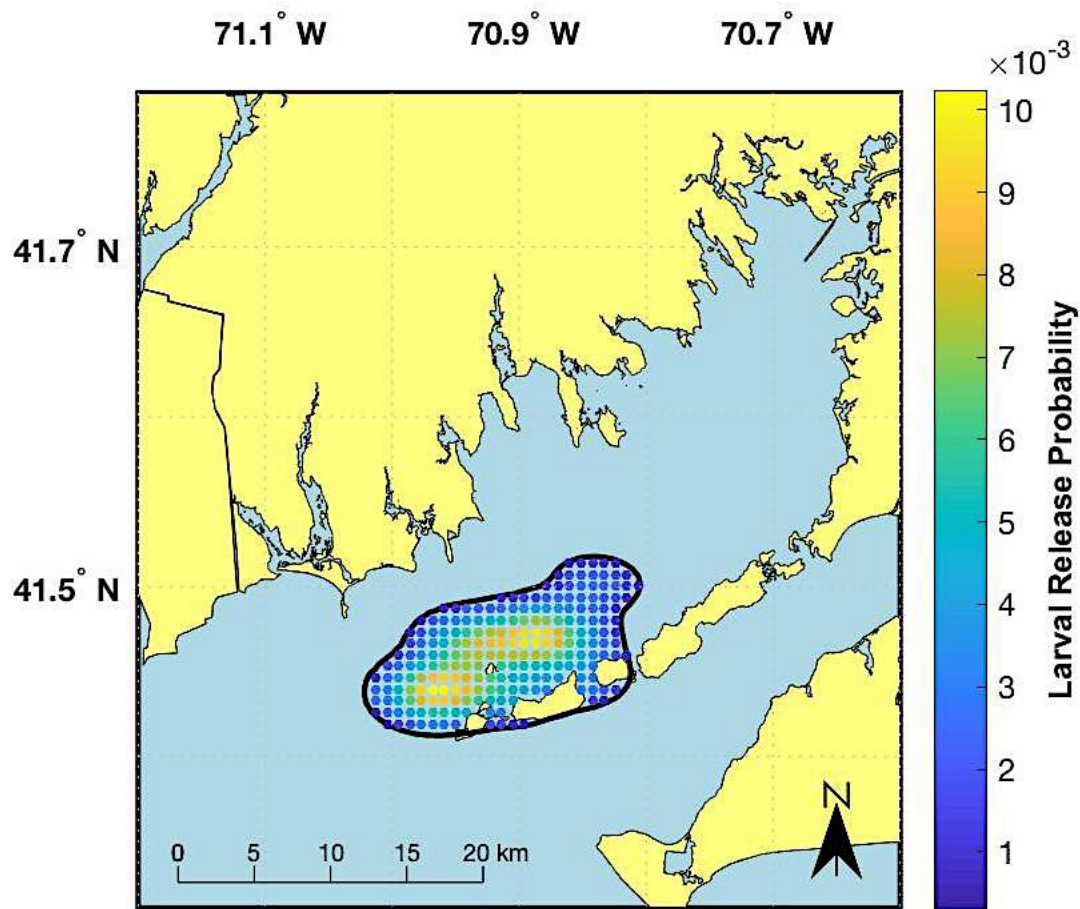
Figures

Figure 1. Left panel: Southeastern Massachusetts (SEMA) coastline with the location of NMFS statistical area 538 (data source: NOAA Northeast Fisheries Science Center, ftp://ftp.nefsc.noaa.gov/pub/gis/), as well as the SEMA region of bottom trawl surveys conducted by MADMF (data source: MADMF). Right panel: Enhanced view of Buzzards Bay with locations of three stations with long-term water temperature observations. The Bay mouth and Cleveland Ledge stations are operated by MADMF and record bottom temperature. The Woods Hole station, currently operated by NOAA's National Ocean Service, records sea surface temperature.

Figure 2. Top panel: Commercial lobster landings from NMFS statistical area 538 (bars) and spawning stock biomass (*SSB*) estimated from spring bottom trawl surveys conducted by MADMF in the SEMA region (dotted line) (data source: MADMF). Bottom panel: Annual deviations from the time series mean number of degree-days above 19°C calculated from sea surface temperatures recorded at Woods Hole, MA (2012 data unavailable; data sources: NOAA National Data Buoy Center, https://www.ndbc.noaa.gov/station_page.php?station=bzbm3 and Woods Hole Oceanographic Institution Data Library and Archives, http://dlaweb.whoi.edu/water_temperatures/water_temp.php). The degree-days value for each year represents the sum of amounts by which daily averages exceeded 19°C. The time series mean is 218 degree-days.
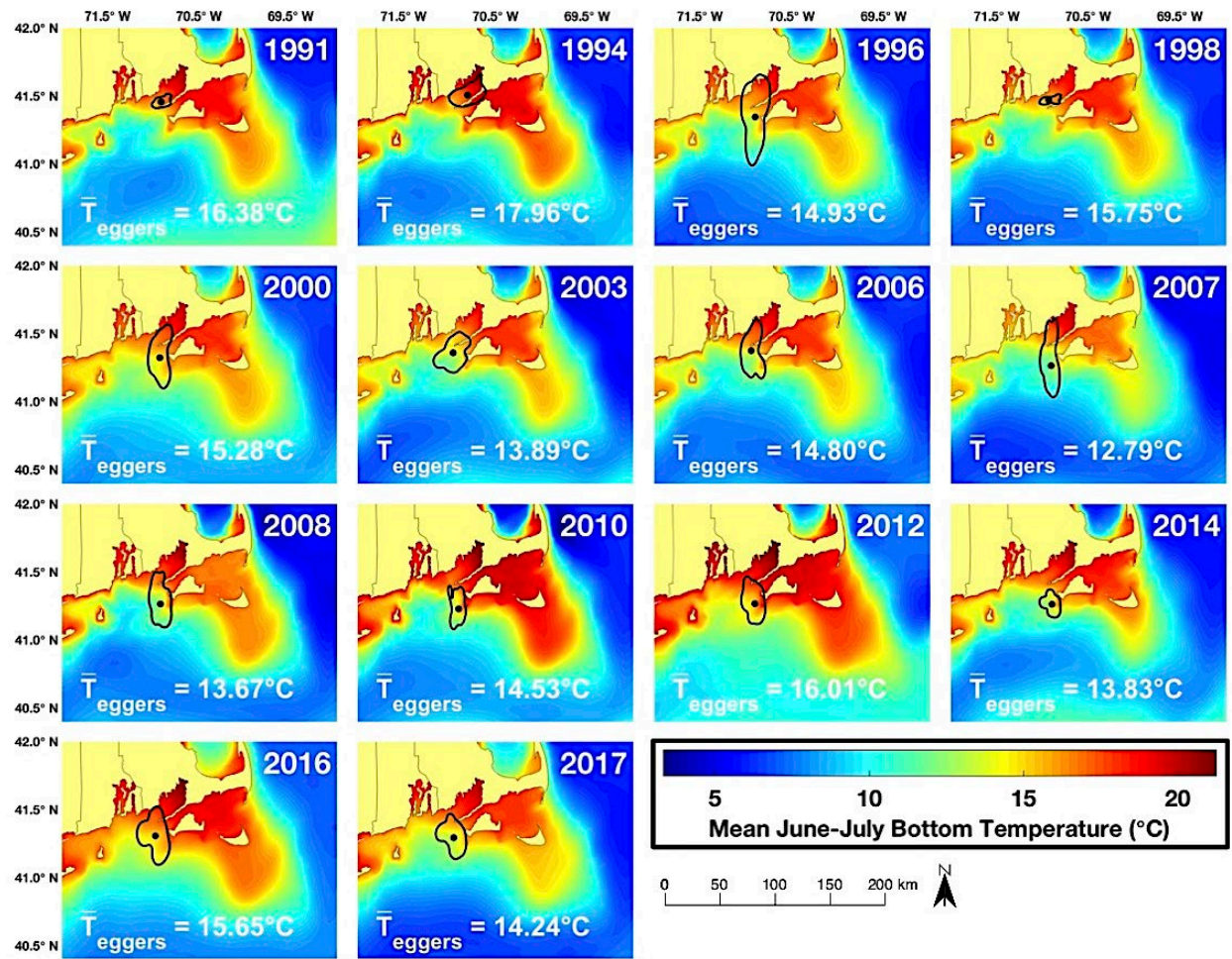
Figure 3. In computing transport success, post-larval lobster settlement was restricted to locations in Buzzards Bay with depths between 2 and 18 meters and with surficial sediments dominated by rock. The Buzzards Bay settlement domain polygon, 18-meter isobath, and rock-dominant classification are shown (surficial sediments data source: Massachusetts Ocean Resource Information System, http://maps.massgis.state.ma.us/map_ol/moris.php; see Foster et al., 2016). Also shown are the locations of five suction sites sampled annually as part of the ALSI monitoring program.
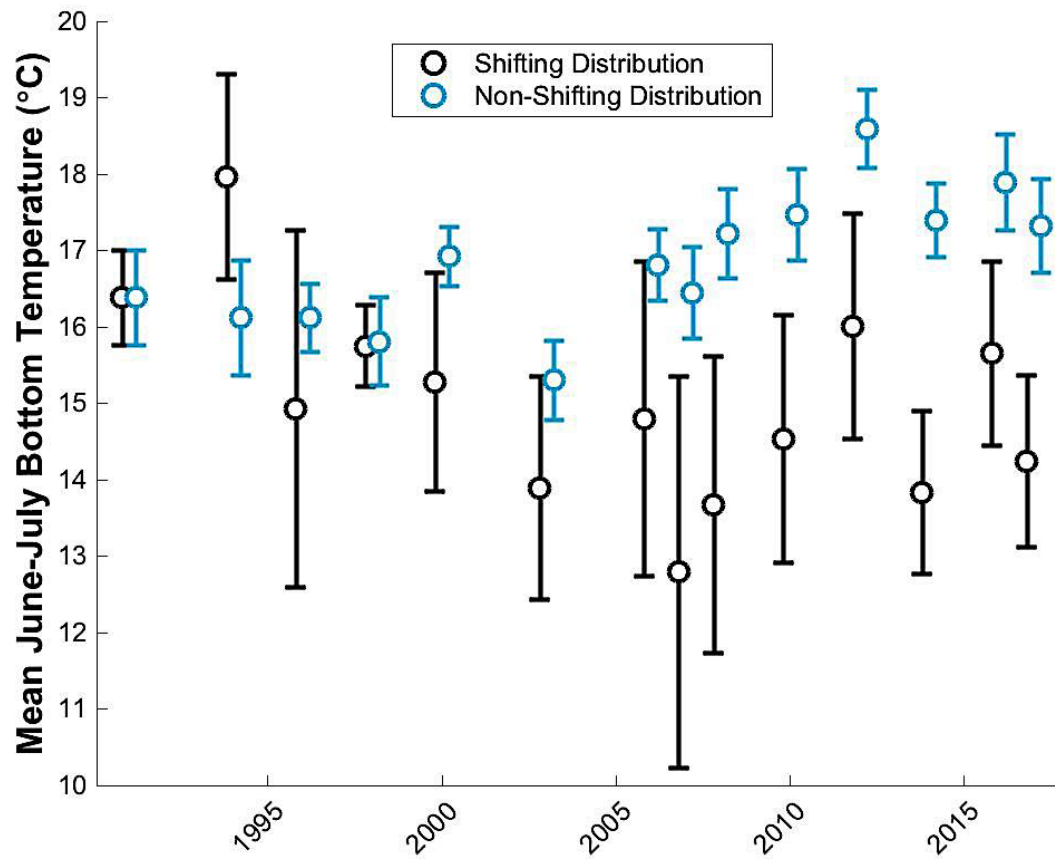
Figure 4. Modeled larval release probability applied to distinct release locations for an example model year (1991). Release probability has been interpolated from a probability density function (PDF) characterizing the spatial distribution of late-stage and spent egg-bearing lobsters in commercial sampling data collected by MADMF. The release boundary (solid black line) was determined as the boundary containing the uppermost 95% of this original probability.
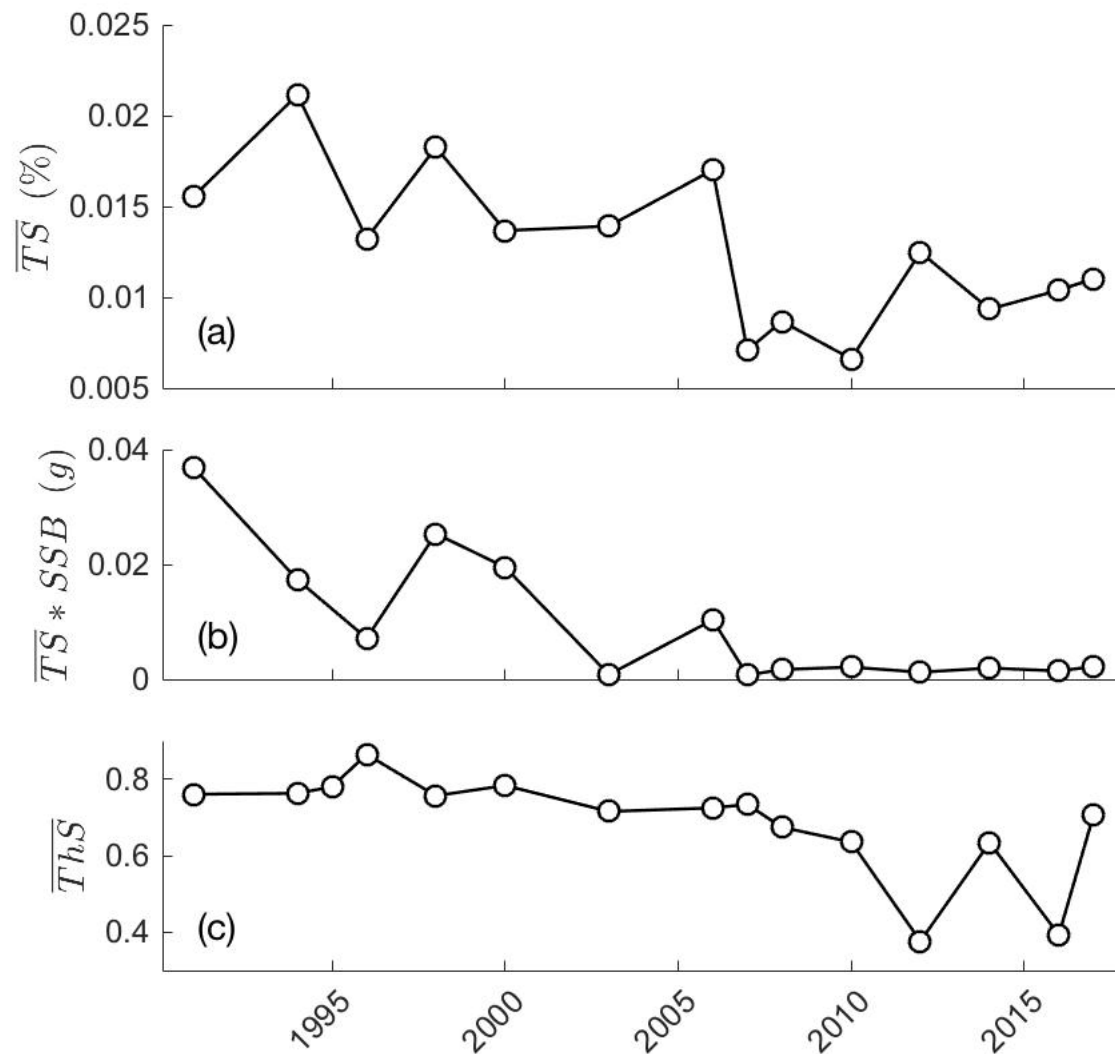
Figure 5. Top panel shows density (individuals per m^2) of EBP lobsters from suction surveys conducted at five ALSI sites in Buzzards Bay (bars; data source: MADMF; 2015-2017 indicate zero density) and number of degree-days above 19°C calculated from bottom temperatures recorded at Cleveland Ledge (dotted line; data source: MADMF; 2004-2005 not included due to an incomplete temperature record). Bottom panel shows natural log transformed EBP density from the five sites plotted against the number of degree-days above 19°C at Cleveland Ledge, with least squares regression shown (dashed line; 2004 and 2005 not included in regression or correlation). Pearson's correlation coefficient, $r = -0.5858$; $P = 0.0084$.
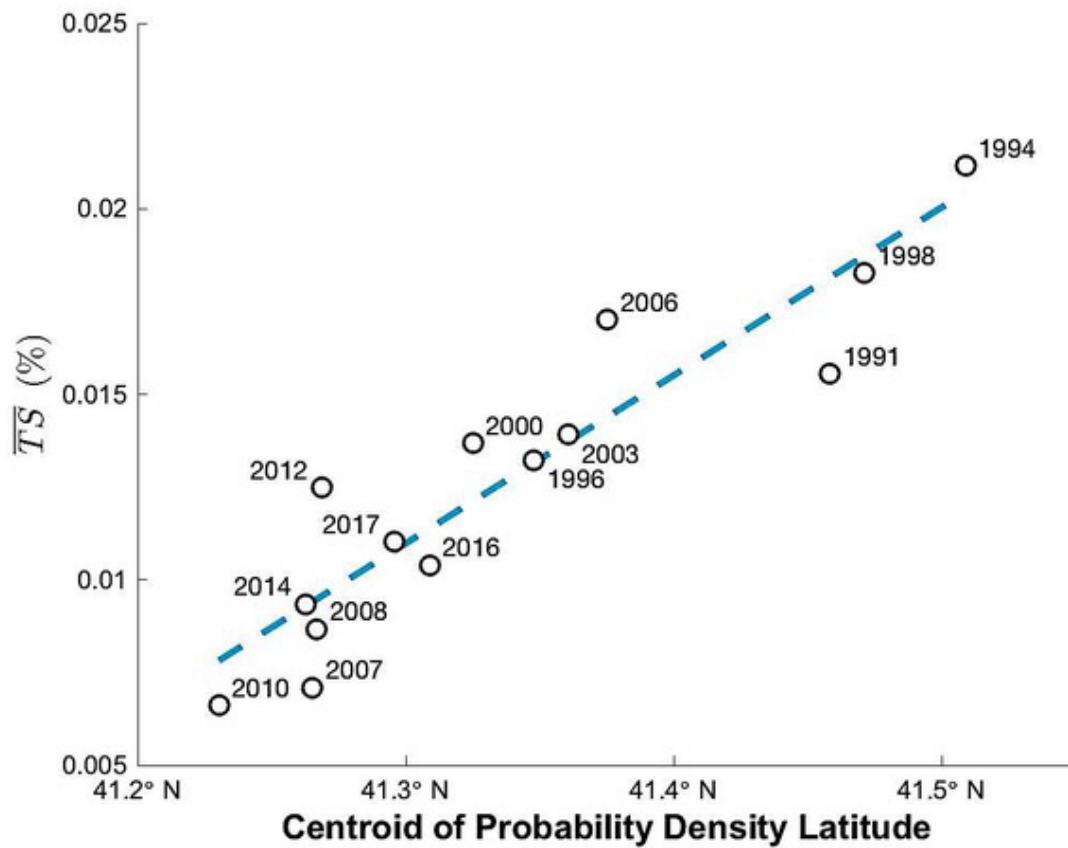
Figure 6. Mean June 1 – July 31 bottom temperature from GOM-FVCOM model configuration refined with *in situ* temperature data. The probability-weighted average temperature over larval release areas (black boundaries) is denoted by $\overline{T}_{eggers}$. The centroid of the larval release probability within each release area is marked by a black dot.

Figure 7. Mean (± SD) June 1 – July 31 bottom temperatures for an offshore-shifting distribution of egg-bearing female lobsters (observed condition) and a non-shifting distribution (theoretical condition; 1991 boundary assumed for all years). The error bars represent the spatial standard deviation in average June-July temperatures.

Figure 8. Summary, in the form of spatial and yearly averages, of the transport success and thermal suitability calculations: (a) yearly averaged transport success ($\overline{TS}$), (b) $\overline{TS}$ x *SSB*, where spawning stock biomass (*SSB*) is assumed to be proportional to the overall supply of larvae released in the SNE region, and (c) yearly and spatially averaged thermal suitability index ($\overline{ThS}$). One-tailed Mann-Kendall tests confirmed significant downward trends: P(a) = 0.0187; P(b) = 0.0244; P(c) = 0.0008. Taken together, the trends indicate degrading probability of larval transport to the designated settlement area (Figure 3) and degrading thermal suitability for EBP survival within that area.

Figure 9. The yearly averaged transport success ($\overline{TS}$) plotted against the latitude of the centroid of the larval release probability of each year (Figure 6). $\overline{TS}$ is strongly correlated (R^2 = 0.86; P < 0.0001) with the centroid latitude (which roughly decreases with distance from shore) implying that the delivery of larvae to near-shore habitat suitable for juvenile settlement declines as the area of larval release shifts offshore.